AGU ADVANCING EARTH AND SPACE SCIENCE

Geophysical Research Letters

RESEARCH LETTER
10.1029/2020GL092031

Key Points:

- An increasing summer interannual surface air temperature (SAT) variability in interior Eastern Antarctica (EA) and the Antarctic Peninsula (AP) simulated in 2051–2099
- An increasing difference in summer interannual SAT between EA and the AP simulated in 2051–2099 than in 1979–2004
- The increasing difference in summer interannual SAT caused by a larger Southern Hemisphere Annular Mode-related circulation anomaly in 2051–2099 than in 1979–2004

Supporting Information:

Supporting Information may be found in the online version of this article.

Correspondence to:

R. Mao,
mr@bnu.edu.cn

Citation:

Mao, R., Kim, S.-J., Gong, D.-Y., Liu, X., Wen, X., Zhang, L., et al. (2021). Increasing difference in interannual summertime surface air temperature between interior East Antarctica and the Antarctic Peninsula under future climate scenarios. *Geophysical Research Letters*, *48*, e2020GL092031. https://doi.org/10.1029/2020GL092031

Received 1 FEB 2021
Accepted 29 JUN 2021

Increasing Difference in Interannual Summertime Surface Air Temperature Between Interior East Antarctica and the Antarctic Peninsula Under Future Climate Scenarios

Rui Mao[1,2,3], Seong-Joong Kim[4], Dao-Yi Gong[1,2], Xiaohong Liu[3], Xinyu Wen[5], Liping Zhang[6,7], Feng Tang[8], Qi Zong[1,2], Cunde Xiao[1], Minghu Ding[9], and Sang-Jong Park[4]

[1]State Key Laboratory of Earth Surface Processes and Resource Ecology, Faculty of Geographical Science, Beijing Normal University, Beijing, China, [2]Academy of Disaster Reduction and Emergency Management, Faculty of Geographical Science, Beijing Normal University, Beijing, China, [3]Department of Atmospheric Science, University of Wyoming, Laramie, WY, USA, [4]Korea Polar Research Institute, Incheon, Korea, [5]Department of Atmospheric and Oceanic Sciences, School of Physics, Peking University, Beijing, China, [6]National Oceanic and Atmospheric Administration/Geophysical Fluid Dynamics Laboratory, Princeton University, Princeton, NJ, USA, [7]Cooperative Programs for the Advancement of Earth System Science, University Corporation for Atmospheric Research, Boulder, CO, USA, [8]Xinhua Middle School, Shenzhen, China, [9]Institute of Polar Meteorology, Chinese Academy of Meteorological Sciences, Beijing, China

Plain Language Summary Melting of the Antarctic ice sheet and shelf in the future will be influenced by interannual changes in the surface air temperature (SAT) in Antarctica. The SAT changes in Antarctica are related to variations in the Southern Hemisphere Annular Mode (SAM) during the austral summer. The SAM is a dominant pattern of atmospheric variability in the Southern Hemisphere and influences the Antarctic SAT with opposite changes between the northern Antarctic Peninsula (AP) and Eastern Antarctica (EA). To project future changes in the Antarctic SAT, we analyzed historical and future simulations from the Climate Model Intercomparison Project 5 models. We found that the degree of opposite interannual SAT changes between EA and the AP increases in the future due to intensified magnitude of the SAM-related circulation anomalies, and summers of warmer SAT in the northern AP and cooler SAT in EA increase by 4% in the future compared to the historical period. This finding has major consequences for glacier melting in the northern AP in the future because more days of extremely high SAT in the northern AP may occur in the future.

Abstract In this study, using the Climate Model Intercomparison Project 5 (CMIP5) simulations and by empirical orthogonal function (EOF) analysis, the first mode of variability in interannual surface air temperature (SAT) in Antarctica (EOF1) was examined for the period between 1979–2004 and 2051–2099 during the austral summer. The ensemble mean of EOF1 of the CMIP5 models shows a positive SAT anomaly over the northern Antarctic Peninsula (AP) and a negative SAT anomaly over Eastern Antarctica (EA) in both periods. A poleward expansion of the AP positive anomaly and an increase in the negative anomaly over interior EA are expected in 2051–2099, resulting in a larger difference of interannual SAT between interior EA and the AP in 2051–2099 than in 1979–2004. The increasing difference in the interannual SAT is consistent with a larger magnitude of the SAM-related circulation anomalies in the future.

1. Introduction

Recent changes in surface air temperature (SAT) in Antarctica have been widely studied (e.g., Clem et al., 2020; Jun et al, 2020; Marshall, 2007; Marshall & Bracegirdle, 2015; Schneider et al., 2004; Schneider & Steig, 2002; Smith & Polvani, 2017; Turner et al., 2004). Since the mid-twentieth century, there has been a noticeable asymmetry of long-term changes in the annual mean SAT between the Antarctic Peninsula (AP) and Eastern Antarctica (EA) (Smith & Polvani, 2017). The AP experienced statistically significant annual warming during 1958–2012 (Clem & Fogt, 2015; Nicolas & Bromwich, 2014; Turner et al., 2004). However, regarding the high plateau and coastal regions of EA, SAT showed a significant cooling trend in the austral autumn from the 1970s to the early 2000s (Screen & Simmonds, 2012). Over the first two decades of the twenty-first century, the autumn cooling on the high plateau has reversed (Nicolas & Bromwich, 2014; Clem et al., 2020).

The spatial asymmetry of long-term changes in SAT in Antarctica is associated with an increasing trend in the Southern Hemisphere Annular Mode (SAM) (Kwok & Comiso, 2002; Kwon et al., 2020; Marshall et al., 2006; Marshall & Bracegirdle, 2015; Thompson & Solomon, 2002; van den Broeke & van Lipzig, 2004) and in the internal variability (Jun et al, 2020). The SAM is a pattern that involves a zonally symmetric seesaw in sea level pressure and geopotential height between the southern polar region and middle latitudes in the Southern Hemisphere (Gong & Wang, 1999; Thompson & Wallace, 2000). The SAM pattern alters westerly winds around Antarctica (Zheng et al., 2013), locations of blocking (Parsons et al., 2016), the Amundsen Sea Low (Hosking et al., 2016), and the Antarctic temperature (Marshall et al., 2006). There has been a significant increasing trend in the summer SAM since the mid-1960s, which was related to stratospheric ozone depletion during the second half of the twentieth century and an increase in greenhouse gas (GHG) concentrations (Arblaster & Meehl, 2006; Thompson et al., 2011). When the SAM is in a positive phase, SAT is lower in EA and higher in the AP (Marshall & Thompson, 2016; Schneider et al., 2004; Schneider & Steig, 2002; van den Broeke & van Lipzig, 2004). The lower SAT in EA with a positive SAM phase is driven by two causes: suppressed warm air transports from the midlatitudes to EA and local weakening winds at the surface that intensify surface temperature inversion by reducing vertical mixing in the atmosphere (Marshall & Bracegirdle, 2015; Previdi et al., 2013; van den Broeke & van Lipzig, 2004). The higher SAT in the AP with a positive SAM phase results from two mechanisms: deepening Amundsen Sea Low (ASL) and the Föhn effects. The deepening ASL enhances onshore flows of warmer maritime air toward the western AP. In addition to the deepening ASL, an increase in zonal winds across the AP associated with the increase in the SAM leads to warming in the northeastern AP by the Föhn effects (Clem et al., 2016; Orr et al., 2008).

Some studies have examined the projected future Antarctic SAT under representative concentration pathway (RCP) scenarios in the fifth Climate Model Intercomparison Project (CMIP5) (Palerme et al., 2017; Tang et al., 2018). These studies indicated a SAT increase over whole Antarctica from 1.0°C (3.9°C) for the scenario RCP 2.6 (RCP 8.5) at the end of the 21st century. Lee et al. (2017) suggested that more ice-free area will emerge in the AP and along the East Antarctic coastline in the future. Although whole Antarctica will be warmer in the future under warming scenarios, regional differences in interannual SAT changes over Antarctica under warming scenarios have not been examined in previous studies. The goal of this study is to examine how regional differences in interannual SAT variations over Antarctica will occur in response to increasing greenhouse gases. To show regional differences in interannual SAT changes, we analyzed the empirical orthogonal function of detrended seasonal SAT and obtained the first mode of interannual SAT variability in Antarctica, which explains the largest portion of SAT variance in Antarctica and is linked to large-scale climate patterns, such as SAM (Clem et al., 2017; Jun et al, 2020; Yu et al., 2011). Then, we compared the first mode of interannual SAT variability from the past decades to the future in Antarctica. This study focuses on the austral summer (December to the following February) because of the following reasons: (a) the Antarctic coasts and shelves undergo snow and ice melting in the austral summer (Torinesi et al., 2003); (b) the SAM is most zonally symmetric and has the most widespread impact on Antarctic temperatures in the austral summer, with more stations of significant correlation between the SAM and SAT in Antarctica (Fogt et al., 2012; Marshall & Bracegirdle, 2015); and (c) a weak influence of tropical Pacific sea surface temperature on the SAT in the AP was found in the austral summer (Clem et al., 2016, 2020).

The remainder of this manuscript is organized as follows. In Section 2, we introduce meteorological observations, reanalysis data, and simulations of the CMIP5 and describe the methods employed in this work. In Section 3, the first mode of interannual SAT variability in Antarctica in 1979–2004 and 2051–2099 is examined using observations, reanalysis data, and CMIP5 simulations under the RCP4.5 and RCP8.5 scenarios (Taylor et al., 2012). Compared to the first mode of interannual SAT variability in 1979–2004, an expansion of positive anomalies in the AP and increased negative anomalies in interior EA in 2051–2099 are identified. The possible cause of the increase in regional differences of interannual SAT between interior EA and the AP in 2051–2099 is addressed in Section 4. Finally, the summary and conclusion are presented in Section 5.

10.1029/2020GL092031

2. Data and Method

In this study, to show the first mode of observed SAT in Antarctica during 1979–2004, monthly SAT from the Scientific Committee on Antarctic Research (SCAR) Reference Antarctic Data for Environmental Research (READER) project and the European Centre for Medium-Range Weather Forecasts Interim (ERA-Interim) Reanalysis data set were used (Dee et al., 2011; Turner et al., 2004). The READER provides monthly mean values of standard meteorological parameters for 26 Antarctic stations during 1979–2006 (available online at http://www.antarctica.ac.uk/met/READER/). After removing stations that had at least one missing record of SAT in 1979–2004, 13 stations were analyzed in this study, which were mainly distributed along the coastline of Antarctica. In addition to the READER data, SATs in 1979–2005 from the ERA-Interim Reanalysis data set with a resolution of 0.75° × 0.75° were examined because they were reported to be better than other reanalysis data sets in studies of Antarctic climate (Bracegirdle & Marshall, 2012; Bromwich & Fogt, 2004; Xie et al., 2016; Yu et al., 2011). Monthly SATs were averaged for the austral summer (December, January, and February of the following year) months.

To obtain the first mode of SAT variability in Antarctica during future decades, CMIP5 simulations (2051–2099 for both the RCP4.5 and 8.5 scenarios) were examined. The SAT in the CMIP5 simulations for a historical period (1979–2005) was also examined to derive the difference in the first mode of interannual SAT variability in Antarctica between past and future decades. Monthly SATs in the simulations were aggregated for the austral summer by averaging them during 1979–2005 and 2051–2099. In addition, the geopotential height (H500) and zonal wind (U500) at the 500 hPa level in 1979–2005 and 2051–2100 in CMIP5 were analyzed to explain the difference in the first mode of interannual SAT variability in Antarctica between 1979–2004 and 2051–2099. The CMIP5 models were selected on the basis of data availability and model diversity, including those with higher horizontal and vertical resolutions and with biological and chemical processes (Table S1) (Zheng et al., 2013).

Interannual changes in SAT explained a large portion of SAT variability in Antarctica, with a ratio of more than 80% in historical observations made for the period 1979–2004, 90% for 2051–2099 under the RCP4.5 scenario, and more than 50% for 2051–2099 under the RCP8.5 scenario (Figure S1). In this study, thus, we examined the first mode of interannual variability of SAT in Antarctica that was retrieved by an empirical orthogonal function (EOF) analysis (Wilks, 2006). The first mode of interannual SAT variability (EOF1) explains the largest variance and is distinguishable from its neighboring EOFs following North et al. (1982). The detrended SAT was employed for the EOF analysis and was weighted by multiplying the square root of the cosine of the latitude prior to the EOF analysis. Note that the detrended seasonal SAT from the READER data was not weighted in the EOF analysis in order to show the results at the South Pole.

3. Results

3.1. EOF1 of Interannual SAT Variability in 1979–2004 and 2051–2099

Figure 1a shows the EOF1 of interannual SAT variability derived from the READER data in 1979–2004. Negative anomalies are dominant in EOF1. Of all the 13 stations, 10 stations showed negative anomalies from the South Pole to coastal regions, with magnitudes less than −0.3. Positive anomalies are sparse, mainly located in the northern AP with magnitudes of 0.2–0.3. EOF1 explains 56% of the detrended SAT variance in Antarctica. The ERA-Interim Reanalysis data set reproduces the EOF1 of detrended SAT variability from the READER data, that is, negative anomalies in Antarctica with the maximum anomalies over the high plateau in EA and positive anomalies in the AP and over the Bellingshausen Sea (Figure 1b). The variance explanation of EOF1 derived by the ERA-Interim Reanalysis data set is 42%. The similarity in EOF1 derived by the two data sets is supported by a high correlation of the first principal component of the two data sets with a correlation coefficient of 0.96, significant at the 95% confidence level (Figure S2).

Figure S3 shows the EOF1 of interannual SAT variability derived from the CMIP5 models in 1979–2004. Most models show good skills in simulating the EOF1 of interannual SAT variability derived by the READER data and the ERA-Interim Reanalysis data set, that is, negative anomalies in Antarctica with centers in EA and positive anomalies in the AP, the Weddell Sea, the Bellingshausen Sea, and the Amundsen Sea with a variance explanation of ∼40% as in the observation. To highlight the key feature of the EOF1s derived by

10.1029/2020GL092031

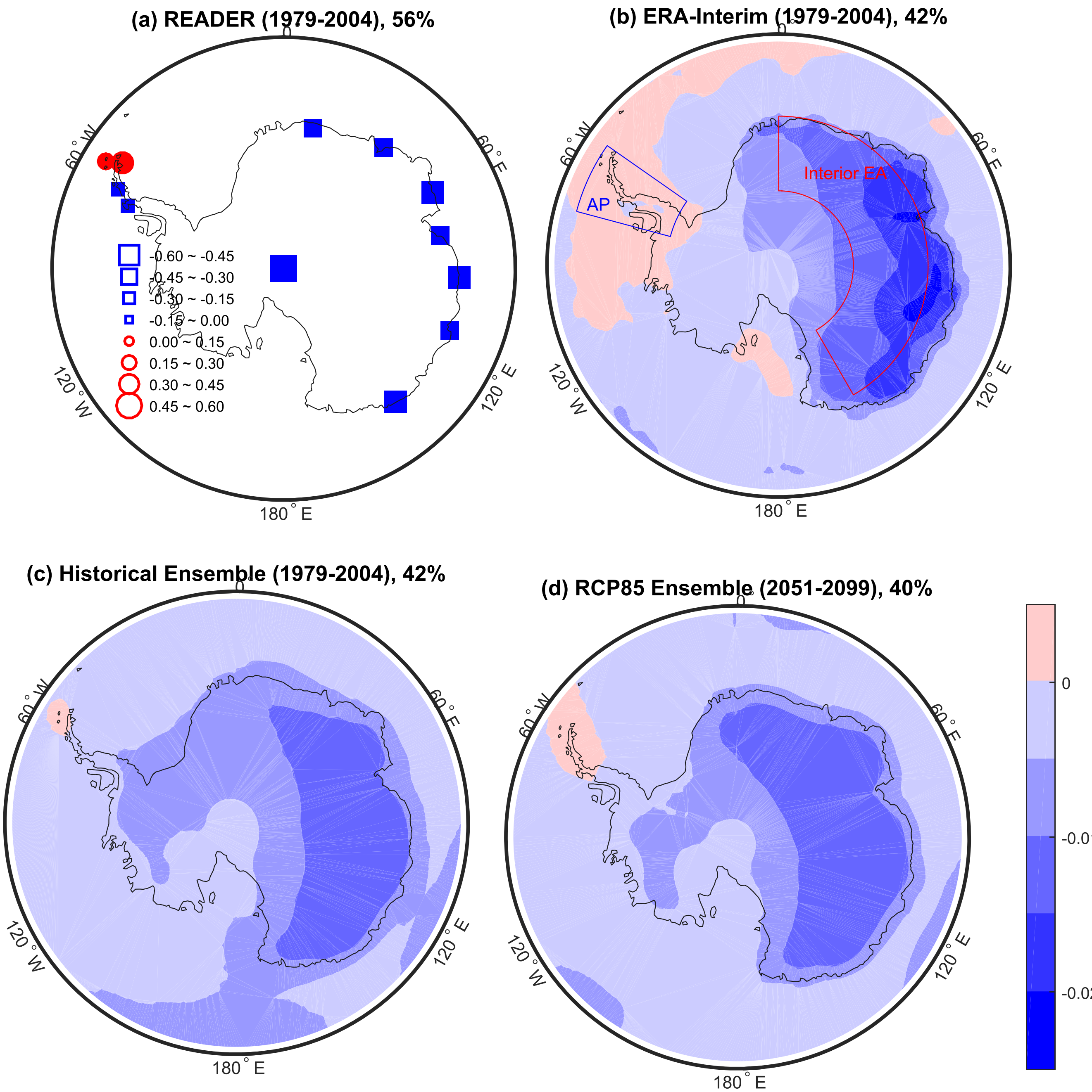

Figure 1. The first mode (EOF1) of variability of detrended surface air temperature (SAT) in the austral summer during 1979–2004 derived from the READER (a) the ERA-Interim Reanalysis data set (b) in Antarctica. (c and d) are multiple-model means of the EOF1 of detrended SAT variability in the austral summer derived by CMIP5 models in 1979–2004 and 2051–2099 under the RCP8.5 scenario, respectively. The interior Eastern Antarctica (EA) and Antarctic Peninsula (AP) in (b) indicate the domain of EA and the AP, respectively.

the CMIP5 models, a multi-model means of EOF1s of all models were obtained by averaging the EOF1s, showing negative anomalies in Antarctica with the maximum anomalies over the high plateau in EA and positive anomalies in the northernmost areas of the AP (Figure 1c).

Prior to deriving the EOF1 of interannual SAT variability in the future, we first evaluated the performance of the CMIP5 models in reproducing the EOF1 of interannual SAT variability in 1979–2004 in Antarctica (Taylor, 2001). It was found that 17 models had correlation coefficients exceeding 0.6 (Figure 2). The standard deviations of these models were close to the observation points in the Taylor diagram, with a range

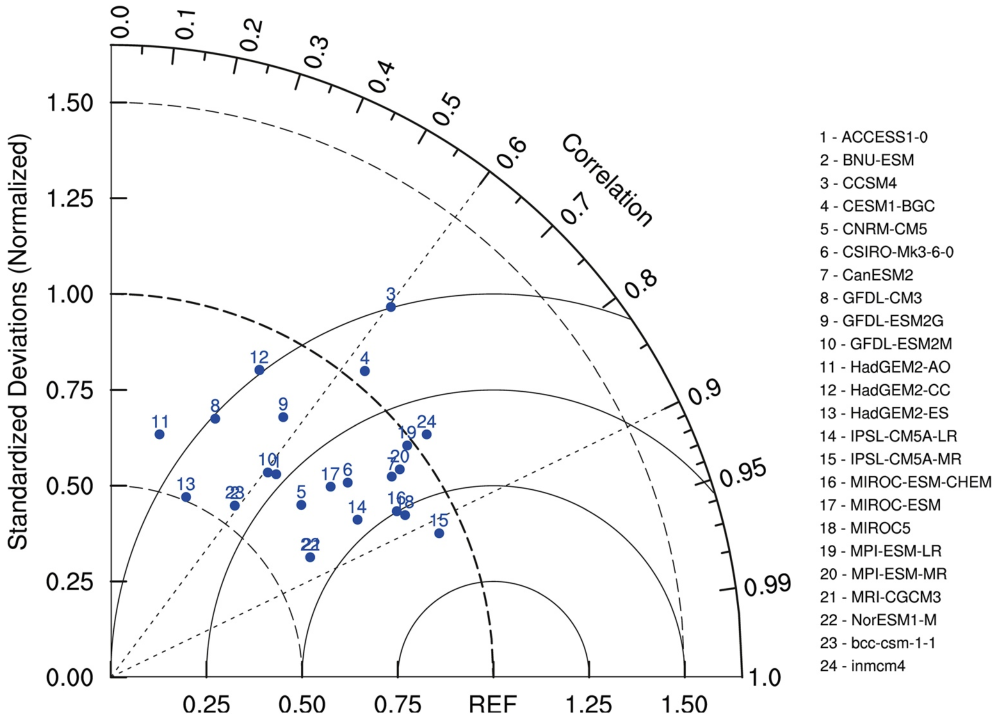

Figure 2. Taylor diagram of model performance in simulating the first mode of variability of detrended surface air temperature (SAT) compared with the ERA-Interim Reanalysis data set during the austral summer for 1979–2004 in Antarctica.

within 50% of the standard deviation of the observation. Nearly all the models showed good skills in reproducing the EOF1 of interannual SAT variability in Antarctica during 1979–2004.

Figures S3 and S4 show the EOF1 of detrended SAT variability in Antarctica derived by the simulations in 2051–2099 under the scenarios RCP4.5 and RCP 8.5, respectively, from the CMIP5. The dominant feature of the EOF1s is a wide range of negative anomalies over high plateau and coastal regions of Antarctica with large magnitudes in EA. In contrast to the negative anomalies in Antarctica, positive anomalies are in the AP or its surrounding oceans such as the Weddell Sea, the Bellingshausen Sea, and the Amundsen Sea. The explained variance of EOF1 of models is within 22%–68%. The multi-model means of EOF1s in 2051–2099 show overall negative anomalies in Antarctica with maximum anomalies in EA, but positive anomalies in the northern AP (Figure 1d for the RCP8.5 scenario and Figure S5 for the RCP4.5 scenario). The difference in the ensemble mean of EOF1s between 1979–2004 and 2051–2099 for the RCP4.5 (Figure S6a) and RCP8.5 scenarios (Figure 3a) shows an expansion of the positive anomalies in the AP to northeast and southeast in 2051–2099 compared to 1979–2004. In the meantime, there are larger negative anomalies in the interior EA with centers between 0°–60°E (90°E–170°E) for the RCP8.5 (RCP4.5) scenario and smaller negative ones along coastal EA. This implies that the magnitude of negative anomalies in interior EA will increase while the positive anomalies on the AP will be stronger and expand especially poleward. In summary, the difference in the ensemble mean of EOF1 between 2051–2099 and 1979–2004 presents a larger variability in interannual SAT in interior EA and the AP in 2051–2099 than in 1979–2004, resulting in an increase in interannual SAT difference between interior EA and the AP in 2051–2099 than in 1979–2004.

3.2. Increase in Interannual SAT Difference Between Interior EA and the AP in 2051–2099

To measure the increase in interannual SAT difference between the AP and interior EA, the difference in detrended SAT between the AP and interior EA (interior EA minus AP) was calculated in 1979–2004 and 2051–2099, respectively, for each model under the RCP4.5 and RCP8.5 scenarios (Figure 4a). The AP and interior EA are enclosed in Figure 1b as AP (75°W–55°W and 62°S–75°S) and interior EA (0°–150°E and 70°S–80°S), respectively. The median of variances of all models increases in 2051–2099 compared to 1979–

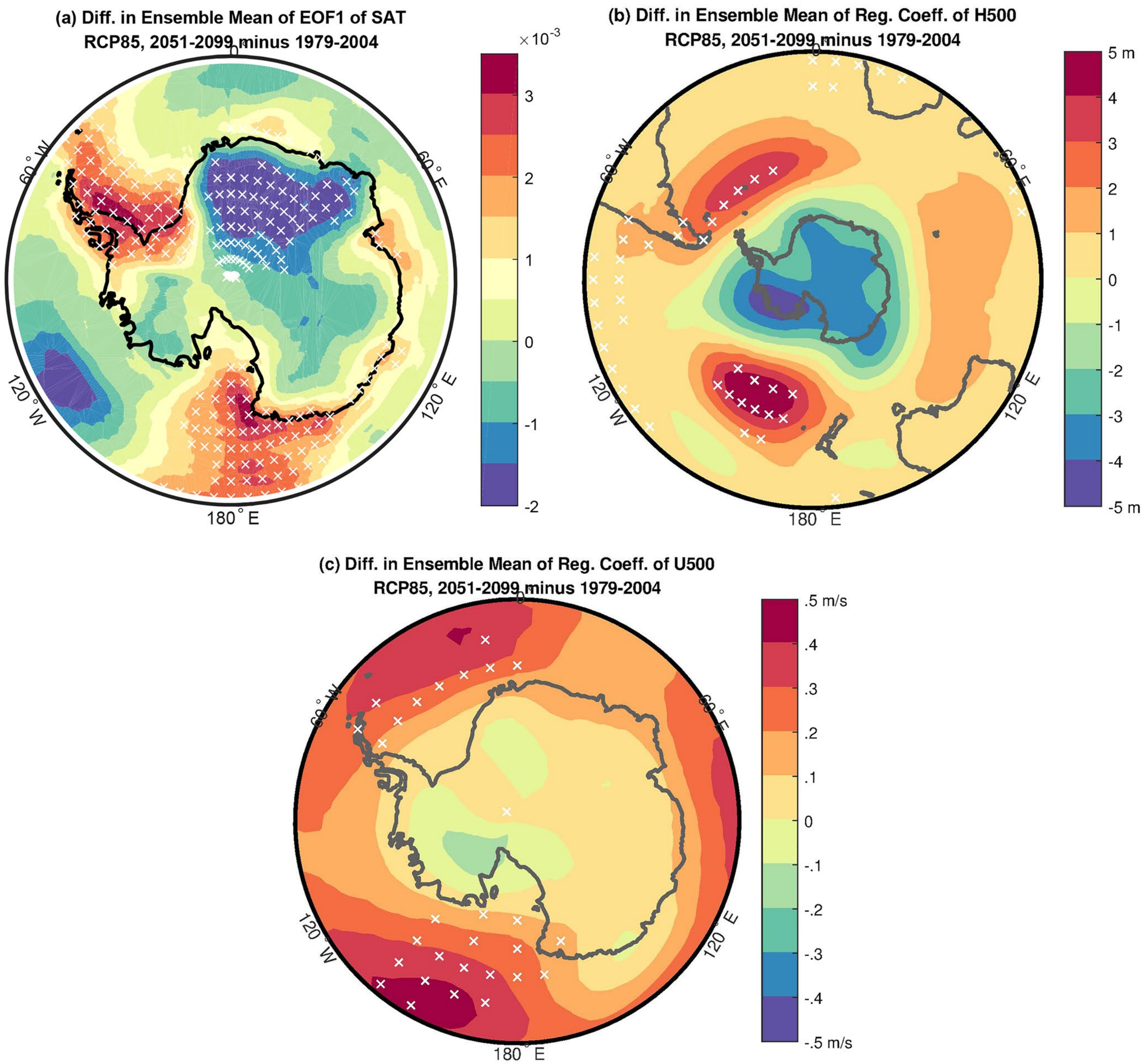

Figure 3. Multi-model means of difference in the first mode of variability of detrended surface air temperature (SAT) (a) and regression coefficient of geopotential height (H500) (b) and zonal-mean zonal wind at 500 hPa (U500) (c) between 1979–2004 and 2051–2099 (2051–2099 minus 1979–2004) for the austral summer. The SAT and H500 (U500) in 2051–2099 are from simulations of CMIP5 models under the RCP8.5 scenario. The regression coefficient of H500 (U500) is obtained by regressing H500 (U500) against the standard deviation of the principal component for each CMIP5 model. The significant difference at the 95% confidence level (Wilcoxon rank-sum test) is indicated by white hatching.

2004 (0.02°C^2 in 1979–2004, 0.08°C^2 in 2051–2099 for the RCP4.5 scenario, and 0.06°C^2 in 2051–2099 for the RCP8.5 scenario), indicating a more contrasting interannual SAT difference between the AP and interior EA in the future (2051–2099) than in the present years (1979–2004).

There are four combinations of detrended SAT anomalies in the AP and interior EA, that is, positive SAT anomalies in the AP and negative SAT anomalies in interior EA (AP+ and EA−), negative SAT anomalies in the AP and positive SAT anomalies in interior EA (AP− and EA+), positive SAT anomalies in both the AP and interior EA (AP+ and EA+), and negative SAT anomalies in both the AP and interior EA (AP− and EA−). Summers of combined SAT anomalies in the AP and interior EA were counted in the RCP4.5 and RCP8.5 scenarios, and their ratios were compared between 1979-2004 and 2051–2099 for the CMIP5 models

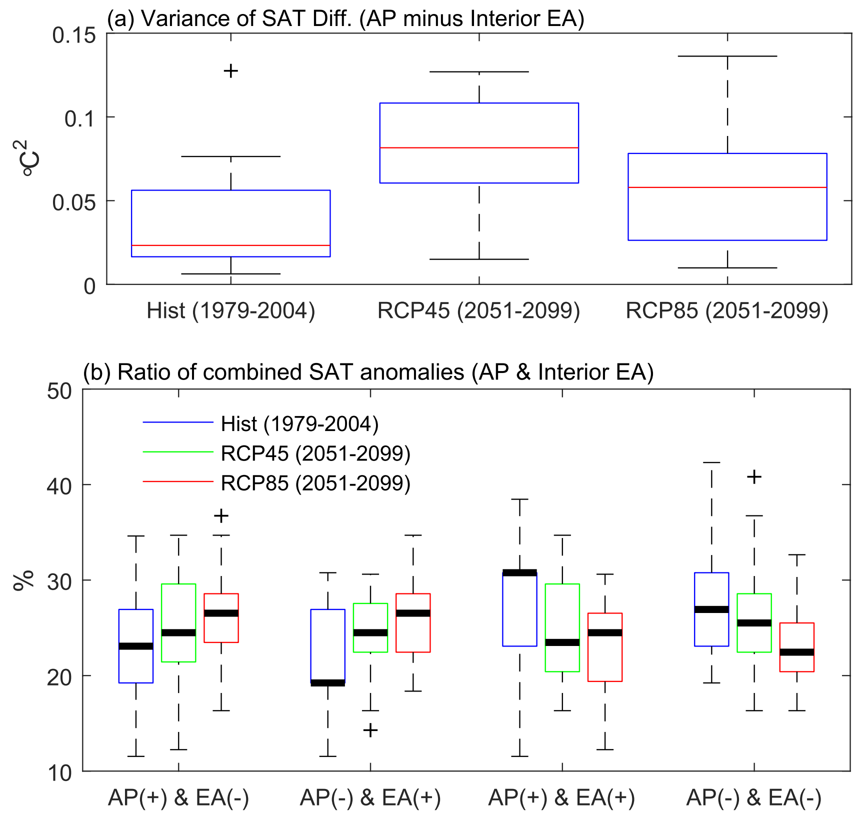

Figure 4. Boxplots of variance of difference in surface air temperature (SAT) between interior East Antarctica (EA) and the Antarctic Peninsula (AP) (EA minus AP) (a) during the austral summer for 1979–2004 and 2051–2099 under the RCP 4.5 and RCP 8.5 scenarios. The median of the variance of SAT difference in 2051–2099 under the RCP4.5 (RCP8.5) scenario is significantly greater than that in 1979–2004 (Wilcoxon rank-sum test). (b) Boxplots of ratio of combined SAT anomalies in the AP and interior EA for 1979–2004 and 2051–2099 under the RCP4.5 and RCP8.5 scenario. The numerator is the number of the selected summers and the denominator is the total number of summers. The crosses indicate outliers of boxplots. The median of the ratio of "AP+ and EA−" ("AP− and EA+") in 2051–2099 under the RCP8.5 is significantly greater than that in 1979–2004 (Wilcoxon rank-sum test).

(Figure 4b). In 1979–2004, the median of the ratio of (EA+ and AP+) and (EA− and AP−) was higher than that of the other two combinations ("EA− and AP+" and "EA+ and AP−"). However, the ratio of "AP+ and EA+" and "AP− and EA−" decreases in 2051–2099, whereas the median of the ratio of "AP+ and EA−" and "AP− and EA+" increases by 4% and 8% in 2051–2099 compared to 1979–2004 in the RCP8.5 scenario, respectively, implying the increase in the difference in interannual SAT between interior EA and the AP during 2051–2099.

3.3. Larger Role of SAM-Related Atmospheric Circulation in the Future

To explain the increase in the interannual SAT difference between the AP and interior EA in 2051–2099, changes in the H500 and U500 associated with the EOF1 (positive anomalies in the northern AP and negative ones in interior EA) were analyzed for the CMIP5 models in the RCP4.5 and RCP8.5 scenarios. For each model and for each scenario, H500 (U500) was regressed against the standard deviation of the principal component in the austral summer in 1979–2004 and 2051–2099, respectively. The difference in the ensemble mean of H500 regressions between 1979–2014 and 2051–2099 shows a negative anomaly in the Amundsen Sea and positive anomalies over the southern portions of the Atlantic Ocean, the Indian Ocean, and the Pacific Ocean (Figure 3b for the RCP8.5 scenario and Figure S6b for the RCP4.5 scenario), indicating a more positive SAM pattern in 2051–2099 than in 1979–2004. The more positive SAM phase is related to enhanced westerly winds in the middle to high latitudes (shown in Figure 3c for the RCP8.5 scenario and Figure S6c for the RCP4.5 scenario), resulting in a cooler SAT over the high interior in Antarctica caused by suppressed meridional air exchange between Antarctica and the midlatitudes and intensified surface temperature inversion. Meanwhile, SAT is higher in the northern AP, which is associated with a deepening of ASL providing warmer maritime air toward the AP and more frequent Föhn effects due to poleward shift of zonal winds across the AP.

As the EOF1 is featured by negative anomalies in the northern AP and positive ones in interior EA, the difference in the ensemble mean of EOF1s can be shown as negative anomalies in the AP and positive ones in the interior EA (figures as shown in Figures 3a and S6a but with values multiplied by −1). In light of this condition, the difference in the ensemble mean of H500/U500 regressions is featured by a more negative SAM phase and an equatorward shift of zonal winds in the middle to high latitudes in 2051–2099 than in 1979–2004 (figures are as shown in Figures 3b, 3c, S6b, and S6c but with values multiplied by −1). Accordingly, the more negative SAM phase is related to a cooler SAT in the AP and a warmer SAT over interior EA in 2051–2099 than in 1979–2004. In summary, the difference in the ensemble mean of EOF1s as in Figures 3a and S6a implies both "higher SAT in the AP and lower SAT in interior EA" and "lower SAT in the AP and higher SAT in interior EA" in 2051–2099 than in 1979–2004 on the interannual timescale, which is consistent with a large magnitude of the SAM-related circulation anomalies in the future.

Finally, we compared the difference in the ensemble mean of EOF1s of interannual SAT variability of CMIP5 models between 1979–2004 and 2051–2099 in the austral summer with that in the austral autumn, winter, and spring under both scenarios (Figures S8 and S9). The results in the austral autumn and winter under the RCP4.5 and RCP8.5 scenarios and that in the austral spring under the RCP8.5 scenario show a similar pattern as that in the austral summer under the RCP4.5 and RCP8.5 scenario, that is, an expansion of positive anomalies in the AP and an increase of negative anomalies in interior EA in 2051–2099 compared to 1979–2004. Under the RCP4.5 scenario, however, the difference in the ensemble mean of EOF1s of CMIP5 models in the austral spring presents a more widespread, positive SAT anomaly over Antarctica in 2051–2099 than in 1979–2004. The question of why spring sees a more widespread, same-sign SAT anomaly than other seasons will be addressed in future works.

4. Summary and Conclusion

In this study, the EOF1 of variability in interannual SAT in Antarctica of 1979–2004 during the austral summer was compared with 2051–2099 in the RCP4.5 and RCP8.5 scenarios. In 1979–2004, the EOF1 of detrended summer SAT variability derived by the observed READER data and the ERA-Interim Reanalysis data set shows negative anomalies in Antarctica, with a center over the high plateau in EA and a positive anomaly in the northern AP. In the RCP4.5 and RCP8.5 scenarios, the ensemble mean of EOF1 of the CMIP5 models in 1979–2004 and 2051–2099 reproduces a similar feature found in observed data with the negative anomaly over the high plateau in EA and the positive anomaly in the northern AP. However, when comparing the ensemble mean of EOF1 between 1979–2004 and 2051–2099 derived from the CMIP5 models, a poleward expansion of the AP warm anomaly, a weakening of the cold anomaly along coastal EA, and an increase in the cold anomaly over interior EA in 2051–2099 is expected compared to 1979–2004. This is proved by an increase in the variance in interannual SAT difference between interior EA and the AP and more frequency of "warmer AP anomaly and cooler interior EA anomaly" and "cooler AP anomaly and warmer interior EA anomaly" at an interannual time scale in 2051–2099 than in 1979–2004.

The increase in the difference in interannual SAT between interior EA and the AP in 2051–2099 is associated with a larger magnitude of the SAM-related circulation anomalies in 2051–2099 than in 1979–2004. For instance, in 2051–2099, the more positive SAM phase in 2051–2099 than in 1979–2009 is related to stronger zonal winds in the middle to high latitudes, resulting in a cooler SAT in interior EA by suppressing meridional air exchange between Antarctica and the midlatitudes, and by intensifying surface temperature inversion. Meanwhile, SAT is higher in the northern AP because of the deepening of the ASL and the increase in zonal winds across the AP, providing more warm air toward the AP and the Föhn effects in the AP (Orr et al., 2008).

In conclusion, the larger interannual SAT difference between the AP and interior EA is expected in the future, especially under the larger greenhouse gas increases associated with a large magnitude of the

SAM-related circulation anomalies. This change might accelerate the ice sheet disintegration in the AP and neighboring regions in the future in addition to ongoing rapid melting of ice shelves like Larsen-C.

Data Availability Statement

Data archiving is underway in mendeley data (doi: 10.17632/gz3ngmmchw.2).

Acknowledgments
The authors thank six anonymous reviewers for their insightful comments. This study was supported by NSFC (41571039), the National Key R&D Program of China (2016YFA0602401), Project PE21030 of the Korea Polar Research Institute, and the Basic Fund of the Chinese Academy of Meteorological Sciences (Grant No. 2021Z006). The authors appreciate the University of Wisconsin-Madison Automatic Weather Station Program and NSF (ANT-1543305).

References

Arblaster, J. M., & Meehl, G. A. (2006). Contributions of external forcings to Southern Annular Mode trends. *Journal of Climate*, *19*, 2896–2905. https://doi.org/10.1175/jcli3774.1

Bracegirdle, T. J., & Marshall, G. J. (2012). The reliability of Antarctic tropospheric pressure and temperature in the latest global reanalyses. *Journal of Climate*, *25*, 7138–7146. https://doi.org/10.1175/jcli-d-11-00685.1

Bromwich, D. H., & Fogt, R. L. (2004). Strong trends in the skill of the ERA-40 and NCEP-NCAR reanalyses in the high and midlatitudes of the southern hemisphere, 1958–2001. *Journal of Climate*, *17*(23), 4603–4619. https://doi.org/10.1175/3241.1

Clem, K. R., & Fogt, R. L. (2015). South Pacific circulation changes and their connection to the tropics and regional Antarctic warming in austral spring, 1979–2012. *Journal of Geophysical Research: Atmospheres*, *120*, 2773–2792. https://doi.org/10.1002/2014jd022940

Clem, K. R., Fogt, R. L., Turner, J., Lintner, B. R., Marshall, G. J., Miller, J. R., & Renwick, J. A. (2020). Record warming at the South Pole during the past three decades. *Nature Climate Change*, *10*, 762–770. https://doi.org/10.1038/s41558-020-0815-z

Clem, K. R., Renwick, J. A., & McGregor, J. (2017). Large-scale forcing of the Amundsen Sea Low and its influence on sea ice and west Antarctic temperature. *Journal of Climate*, *30*, 8405–8424. https://doi.org/10.1175/jcli-d-16-0891.1

Clem, K. R., Renwick, J. A., McGregor, J., & Fogt, R. L. (2016). The relative influence of ENSO and SAM on Antarctic Peninsula climate. *Journal of Geophysical Research: Atmospheres*, *121*, 9324–9341. https://doi.org/10.1002/2016JD025305

Dee, D. P., Uppala, S. M., Simmons, aJ., Berrisford, P., Poli, P., Kobayashi, S., et al. (2011). The ERA-interim reanalysis: Configuration and performance of the data assimilation system. *Quarterly Journal of the Royal Meteorological Society*, *137*(656), 553–597. https://doi.org/10.1002/qj.828

Fogt, R. L., Jones, J. M., & Renwick, J. (2012). Seasonal zonal asymmetries in the Southern Annular Mode and their impact on regional temperature anomalies. *Journal of Climate*, *25*, 6253–6270. https://doi.org/10.1175/JCLI-D-11-00474.1

Gong, D. Y., & Wang, S. (1999). Definition of Antarctic Oscillation index. *Geophysical Research Letters*, *26*, 459–462. https://doi.org/10.1029/1999gl900003

Hosking, J. S., Orr, A., Bracegirdle, T. J., & Turner, J. (2016). Future circulation changes off West Antarctica: Sensitivity of the Amundsen Sea Low to projected anthropogenic forcing. *Geophysical Research Letters*, *43*, 367–376. https://doi.org/10.1002/2015gl067143

Jun, S. Y., Kim, J. H., Choi, J. S. J. K., Kim, B. M., & An, S. I. (2020). The internal origin of the west-east asymmetry of Antarctic climate change. *Science Advances*, *6*, eaaz1490. https://doi.org/10.1126/sciadv.aaz1490

Kwok, R., & Comiso, J. C. (2002). Spatial patterns of variability in antarctic surface temperature: Connections to the Southern Hemisphere Annular Mode and the Southern Oscillation. *Geophysical Research Letters*, *29*, 1705. https://doi.org/10.1029/2002gl015415

Kwon, H., Choi, H., Kim, B. M., Kim, S. W., & Kim, S. J. (2020). Recent weakening of the southern stratospheric polar vortex and its impact on the surface climate over Antarctica. *Environmental Research Letters*, *15*(9), 094072. https://doi.org/10.1088/1748-9326/ab9d3d

Lee, J. R., Raymond, B., Bracegirdle, T. J., Chadès, I., Fuller, R. A., Shaw, J. D., & Terauds, A. (2017). Climate change drives expansion of Antarctic ice-free habitat. *Nature*, *547*, 49–54. https://doi.org/10.1038/nature22996

Marshall, G. J. (2007). Half-century seasonal relationships between the Southern Annular Mode and Antarctic temperatures. *International Journal of Climatology*, *27*, 373–383. https://doi.org/10.1002/joc.1407

Marshall, G. J., & Bracegirdle, T. J. (2015). An examination of the relationship between the Southern Annular Mode and Antarctic surface air temperatures in the CMIP5 historical runs. *Climate Dynamics*, *45*, 1513–1535. https://doi.org/10.1007/s00382-014-2406-z

Marshall, G. J., Orr, A., van Lipzig, N. P. M., & King, J. C. (2006). The impact of a changing Southern Hemisphere annular mode on Antarctic Peninsula summer temperatures. *Journal of Climate*, *19*(20), 5388–5404. https://doi.org/10.1175/jcli3844.1

Marshall, G. J., & Thompson, D. W. J. (2016). The signatures of large-scale patterns of atmospheric variability in Antarctic surface temperatures. *Journal of Geophysical Research: Atmospheres*, *121*, 3276–3289. https://doi.org/10.1002/2015JD024665

Nicolas, J. P., & Bromwich, D. H. (2014). New reconstruction of Antarctic near-surface temperatures: Multidecadal trends and reliability of global reanalyses. *Journal of Climate*, *27*(21), 8070–8093. https://doi.org/10.1175/JCLI-D-13-00733.1

North, G. R., Bell, T. L., Cahalan, R. F., & Moeng, F. J. (1982). Sampling errors in the estimation of empirical orthogonal functions. *Monthly Weather Review*, *110*, 699–706. https://doi.org/10.1175/1520-0493(1982)110<0699:seiteo>2.0.co;2

Orr, A., Marshall, G. J., Hunt, J. C. R., Sommeria, J., Wang, C. G., van Lipzig, N. P. M., et al. (2008). Characteristics of summer airflow over the Antarctic Peninsula in response to recent strengthening of westerly circumpolar winds. *Journal of the Atmospheric Sciences*, *65*(4), 1396–1413. https://doi.org/10.1175/2007JAS2498.1

Palerme, C., Genthon, C., Claud, C., Kay, J. E., Wood, N. B., & L'Ecuyer, T. (2017). Evaluation of current and projected Antarctic precipitation in CMIP5 models. *Climate Dynamics*, *48*(1-2), 225–239. https://doi.org/10.1007/s00382-016-3071-1

Parsons, S., Renwick, J. A., & McDonald, A. J. (2016). An assessment of future Southern Hemisphere blocking using CMIP5 projections from four GCMs. *Journal of Climate*, *29*(21), 7599–7611. https://doi.org/10.1175/jcli-d-15-0754.1

Previdi, M., Smith, K. L., & Polvani, L. M. (2013). The Antarctic atmospheric energy budget. Part I: Climatology and intraseasonal-to-interannual variability. *Journal of Climate*, *26*, 6406–6418. https://doi.org/10.1175/jcli-d-12-00640.1

Schneider, D. P., & Steig, E. J. (2002). Spatial and temporal variability of Antarctic ice sheet microwave brightness temperatures. *Geophysical Research Letters*, *29*, 1964. https://doi.org/10.1029/2002GL015490

Schneider, D. P., Steig, E. J., & Comiso, J. C. (2004). Recent climate variability in Antarctica from satellite-derived temperature data. *Journal of Climate*, *17*, 1569–1583. https://doi.org/10.1175/1520-0442(2004)017<1569:rcviaf>2.0.co;2

Screen, J. A., & Simmonds, I. (2012). Half-century air temperature change above Antarctica: Observed trends and spatial reconstructions. *Journal of Geophysical Research*, *117*, D16108. https://doi.org/10.1029/2012jd017885

Smith, K. L., & Polvani, L. M. (2017). Spatial patterns of recent Antarctic surface temperature trends and the importance of natural variability: Lessons from multiple reconstructions and the CMIP5 models. *Climate Dynamics*, *48*, 2653–2670. https://doi.org/10.1007/s00382-016-3230-4

Tang, M. S. Y., Chenoli, S. N., Samah, A. A., & Hai, O. S. (2018). An assessment of historical Antarctic precipitation and temperature trend using CMIP5 models and reanalysis datasets. *Polar Science*, *15*, 1–12. https://doi.org/10.1016/j.polar.2018.01.001

Taylor, K. E. (2001). Summarizing multiple aspects of model performance in a single diagram. *Journal of Geophysical Research*, *106*(D7), 7183–7192. https://doi.org/10.1029/2000jd900719

Taylor, R., Stouffer, J., & Meehl, G. A. (2012). An overview of CMIP5 and the experiment design. *Bulletin of the American Meteorological Society*, *93*(4), 485–498. https://doi.org/10.1175/bams-d-11-00094.1

Thompson, D. W. J., & Solomon, S. (2002). Interpretation of recent Southern Hemisphere climate change. *Science*, *296*(5569), 895–899. https://doi.org/10.1126/science.1069270

Thompson, D. W. J., Solomon, S., Kushner, P., England, M. H., Grise, K. M., & Karoly, D. J. (2011). Signatures of the Antarctic ozone hole in Southern Hemisphere surface climate change. *Nature Geoscience*, *4*, 741–749. https://doi.org/10.1038/ngeo1296

Thompson, D. W. J., & Wallace, J. M. (2000). Annular modes in the extratropical circulation. Part I: Month-to-month variability. *Journal of Climate*, *13*(5), 1000–1016. https://doi.org/10.1175/1520-0442(2000)013<1000:amitec>2.0.co;2

Torinesi, O., Fily, M., & Genthon, C. (2003). Variability and trends of the summer melt period of Antarctic ice margins since 1980 from microwave sensors. *Journal of Climate*, *16*, 1047–1060. https://doi.org/10.1175/1520-0442(2003)016<1047:vatots>2.0.co;2

Turner, J., Colwell, S. R., Marshall, G. J., Lachlan-Cope, T. A., Carleton, A. M., Jones, P. D., et al. (2004). The SCAR READER project: Toward a high-quality database of mean Ant- arctic meteorological observations. *International Journal of Climatology*, *17*(14), 2890–2898. https://doi.org/10.1175/1520-0442(2004)017<2890:tsrpta>2.0.co;2

van den Broeke, M. R., & van Lipzig, N. P. M. (2004). Changes in Antarctic temperature, wind and precipitation in response to the Antarctic Oscillation. *Annals of Glaciology*, *39*, 119–126. https://doi.org/10.3189/172756404781814654

Wilks, D. S. (2006). *Statistical methods in the atmospheric sciences* (p. 463). San Diego: Academic Press.

Xie, A. H., Wang, S. M., Xiao, C. D., Kang, S. C., Gong, J. X., Ding, M. H., et al. (2016). Can temperature extremes in East Antarctica be replicated from ERA Interim reanalysis? *Arctic, Antarctic, and Alpine Research*, *48*(4), 603–621. https://doi.org/10.1657/aaar0015-048

Yu, L., Zhang, Z., Zhou, M., Zhong, S., Sun, B., Hsu, H., et al. (2011). The intraseasonal variability of winter semester surface air temperature in Antarctica. *Polar Research*, *30*, 6039. https://doi.org/10.3402/polar.v30i0.6039

Zheng, F., Li, J., Clark, R. R., & Nnamchi, H. C. (2013). Simulation and Projection of the Southern Hemisphere Annular Mode in CMIP5 Models. *Journal of Climate*, *26*(24), 9860–9879. https://doi.org/10.1175/jcli-d-13-00204.1